Geotech Geol Eng (2018) 36:665–683
https://doi.org/10.1007/s10706-017-0337-2

TECHNICAL NOTE

Failure Investigation at a Collapsed Deep Open Cut Slope Excavation in Soft Clay

Jiang Hu · Fuheng Ma

Received: 30 November 2016 / Accepted: 14 August 2017 / Published online: 17 August 2017

Abstract Collapse of a 7.08-m-deep open cut excavation for the bank of a navigation lock in sensitive soft clay in Zhejiang, China, is presented in this paper. Cone penetration tests, field vane shear tests (VSTs), and traditional laboratory tests have been performed to investigate the soil properties after the collapse. According to the test results, the soft soil layers of mucky clay and muck have been found to be disturbed because of the effects of the boring holes. For bored concrete piles, the stresses release due to the cut slope, thus its shear strength is much lower than that measured from laboratory tests. The shear strength reduction technique based on a finite-element method program has been used to study the excavation behavior and overall factor of safety (FOS) of the excavated slope considering geometries of original design, later adopted schemes and soil properties associated with various test types. The computed FOS values obtained from VST results are lower than the corresponding recommended values and just a little higher than the limited value. Thus the excavated slope may easily collapse triggered by additional vehicles and surface surcharge loads. The reasons of excavation collapse can be explained as the misuse of soil properties for designers, and inadequate construction process management. The investigation of the failure provides experiences and lessons for the design and construction of similar projects in sensitive soft clay.

Keywords Slope collapse · Deep unsupported open excavation · Sensitive clay · Soil disturbance · Failure mechanism · Finite-element method

1 Introduction

Geologically young, normal consolidated cohesive soft soils are distributed worldwide along coastal areas and around lakes and rivers such as North and Central America (e.g. Mexico Clay, Cancagua or lacustrine sediments; Eastern Canada), Southern Germany, Southern Norway, Central Plain of Thailand, Southeastern China, etc. (Kempfert and Gebreselassie 2006; Wu et al. 2015; Likitlersuang et al. 2013; Arasan et al. 2016). The Quaternary deposits are generally characterized by high water content with high compressibility, high sensitivity, high viscosity, and low shear strength. Construction of engineering and geotechnical structures on soft soils usually involves with excessive settlements, deformations and stability problems (Likitlersuang et al. 2013). However, many excavations were executed for the subway station, building foundation, and navigation and river channel slope also in soft soil with the rapid development of the infrastructure in or around urban areas in the southeast

J. Hu (✉) · F. Ma
State Key Laboratory of Hydrology-Water Resources and Hydraulic Engineering, Nanjing Hydraulic Research Institute, Nanjing 210029, China
e-mail: huj@nhri.cn

coastal region of China (Wu et al. 2015; Chen et al. 2015). The planning, design and construction of excavations and foundations in soft to very soft soils is always a difficult and challenging assignment to engineers because the failure of excavations usually leads to large property losses or even loss of lives.

In recent years, several incidents involving collapses of excavations in soft soil have been reported, and the main reason for these was considered to be the insufficient strength of the soil (Likitlersuang et al. 2013; Chen et al. 2015; Zhang et al. 2015). In fact, the factors that are most important in controlling the excavation behavior include the type and strength of the soil around and beneath the excavation, as well as the excavation and supporting procedure, the groundwater condition, and environmental conditions (Kempfert and Gebreselassie 2006; Tan et al. 2015). Therefore, evaluation of the excavation behavior in soft soil is an issue of great concern to practical engineers. With expansion of the city, many of the newly planned projects exist in areas where sufficient open land is available around the excavation site (Kempfert and Gebreselassie 2006; Irfan et al. 2013; Keawsawasvong and Ukritchon 2017). In such areas, unsupported open excavations by maintaining appropriate side slopes offer economical solution. Open excavations are complicated in a soil-structure system, and representative failures documented in case histories are very useful to investigate the factors that influence the safety of excavations and to also improve excavation design.

The area around the rivers and along coastal areas in Southeastern China consists of a thick layer of sensitive organic deposit (Wu et al. 2015). This paper presents a collapse of a deep open cut excavation for the bank of the Jinqingxin Navigation Lock project, which locates in Taizhou and was constructed over a soft clay deposit. Two zones of slope collapse were observed during and after sloped excavation construction. The project backgrounds, such as site condition, design arrangement and later change, construction stages, and slope collapses, are introduced firstly. Then, in-situ field investigation and numerical modeling results are analyzed in detail. The objectives of this article are as follows: (1) to investigate the soil properties of muck and mucky clay under the construction disturbance investigated by cone penetration tests (CPTs) and field vane shear tests (VSTs), with a focus on the relationship between the in-situ field and laboratory tests; (2) to reveal the failure mechanism of the unsupported open cut slope after the excavation emphasizing the design and construction process; (3) to provide engineers and contractors with a good case history of a failure of deep open cut excavation in sensitive soft clay, and to give some suggestions.

2 Project Background

2.1 Site Conditions

The construction site is located around Jingqing River in Taizhou–Wenzhou–Huangyan Plain, as shown in Fig. 1. The region belongs to low land with an altitude of 2.5–3.5 m. The delta consists of an alluvial plain

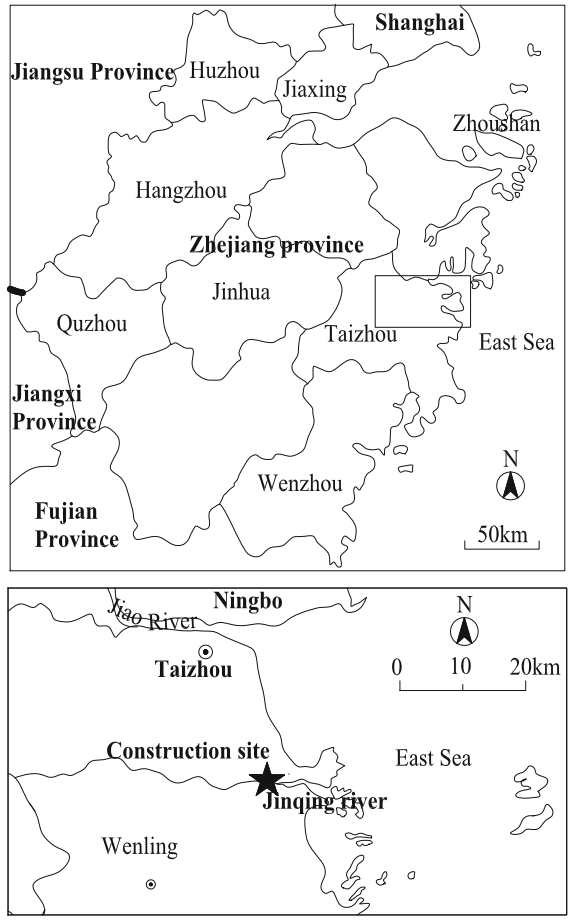

Fig. 1 Location of the project site in Taizhou, Zhejiang province, China

filled with sedimentary soils, especially a thick soft to very soft clay layer deposit down the top. The ground water level fluctuates between 0.5 and 1.0 m below the ground surface.

Before excavation, soil conditions at the site were explored by a series of field exploration programs and laboratory tests. Field exploration and laboratory tests show that the soils, down to a maximum drilling depth of approximately 60.0 m, can be roughly divided into 3 layers and 8 sub-layers. The physical and mechanical properties of the soil deposit associated with the testing types are summarized in Table 1. The subsurface soils consist of a thin layer of fill (layerI-1, rQ) in the upper 1.0 m below ground level (GL-1.0 m) followed by a clay layer (layer I-2, al-mQ4) to the depth of approximately GL-3.5 m. Beneath the layer I2 is a layer of very soft mucky clay (layer II-1, mQ4) to the depth of GL-13.0 m. From GL-13.0 m to GL-23.3 m, there is also a layer of very soft muck (layer II-2, mQ4) which is followed by a thin layer of mucky clay (layer II-3, mQ4). Below the layer II-2 is a layer of silty clay (layer III-1, al-mQ4) to the depth of GL-31.4 m. From GL-31.4 m, there is clay (layer III-2, al-mQ4) and silt clay layers (layer III-3, al-mQ4) successively, whose depths were not explored determinately. It is believed from the experience that it extends at least up to a depth of 60 m below the ground surface (GL-60.0 m). The field exploration indicated that the main soils of the site are basically soft clayey soils that feature relatively high water content, high void ratio, high compressibility, and low strength. This is also typical for many other project sites around rivers and along coastal areas in Zhejiang province in Southeastern China. The results listed in Table 1 were used in the original design.

2.2 Initial Design Arrangement and Later Change

The plan for the Jinqingxin Navigation Lock project site is presented in Fig. 2. The Lock is composed of five sections: upstream approach channel, upper lock head, lock chamber, down lock head and downstream approach channel.

The upstream approach channel, the lock chamber, and the downstream approach channel have the similar compound geometry. In Fig. 3, the geometry of the upstream approach channel is presented with an "averaged" profile of subsurface stratigraphy interpreted from a series of borings conducted at the site.

Table 1 Soil properties for original design at the project site

Stratum	w (%)	γ (kN/m^3)	s_r (%)	e_0	w_l (%)	w_p (%)	I_p	I_l	k_v (cm/s)	k_h (cm/s)	c_v (MPa^{-1})	E_s (MPa)	c_q (kPa)	φ_q (°)	c_{cq} (kPa)	φ_{cq} (°)
I2: clay	41.1	18.0	99.5	1.133	43.4	24.6	18.2	0.81	1.39e−6	1.12e−6	0.862	2.69	18.0	5.0	25.0	17.0
II1: mucky clay	51.4	17.2	100.0	1.446	46.2	25.4	20.6	1.25	2.84e−6	5.08e−6	1.294	1.88	8.0	3.0	11.0	15.0
II2: muck	56.4	16.9	100.0	1.560	51.1	27.7	23.4	1.22	4.54e−7	1.20e−5	1.396	1.82	11.0	3.2	14.0	14.0
II3: mucky clay	45.5	17.7	100.0	1.263	46.1	24.9	21.2	0.89			0.767	2.87	18.0	5.0	20.0	14.0
III1: silty clay	32.6	19.1	99.7	0.894	32.8	19.7	13.0	1.04	8.82e−6	6.14e−5	0.457	4.23	14.0	11.0	22.0	21.0
III2: clay	36.6	18.7	99.8	1.009	40.4	23.0	18.3	0.77	4.59e−7	2.04e−6	0.622	3.33	21.0	6.0	23.0	17.0
III3: silty clay	31.8	19.1	100.0	0.874	35.8	20.9	14.9	0.64			0.391	4.70			25.0	19.0

w, Water content; γ, unit weight; s_r, saturation degree; e_0, void ratio; w_l, liquid limit; w_p, plastic limit; I_p, plasticity index; I_l, liquidity index; k_v, vertical permeability coefficient; k_h, horizontal permeability coefficient; c_v, coefficient of compressibility; E_s, compressibility modulus; c_q, cohesion of quick direct shear test; φ_q, internal friction angle of quick direct shear test; c_{cq}, cohesion of consolidated quick direct shear test; φ_{cq}, internal friction angle of consolidated quick direct shear test

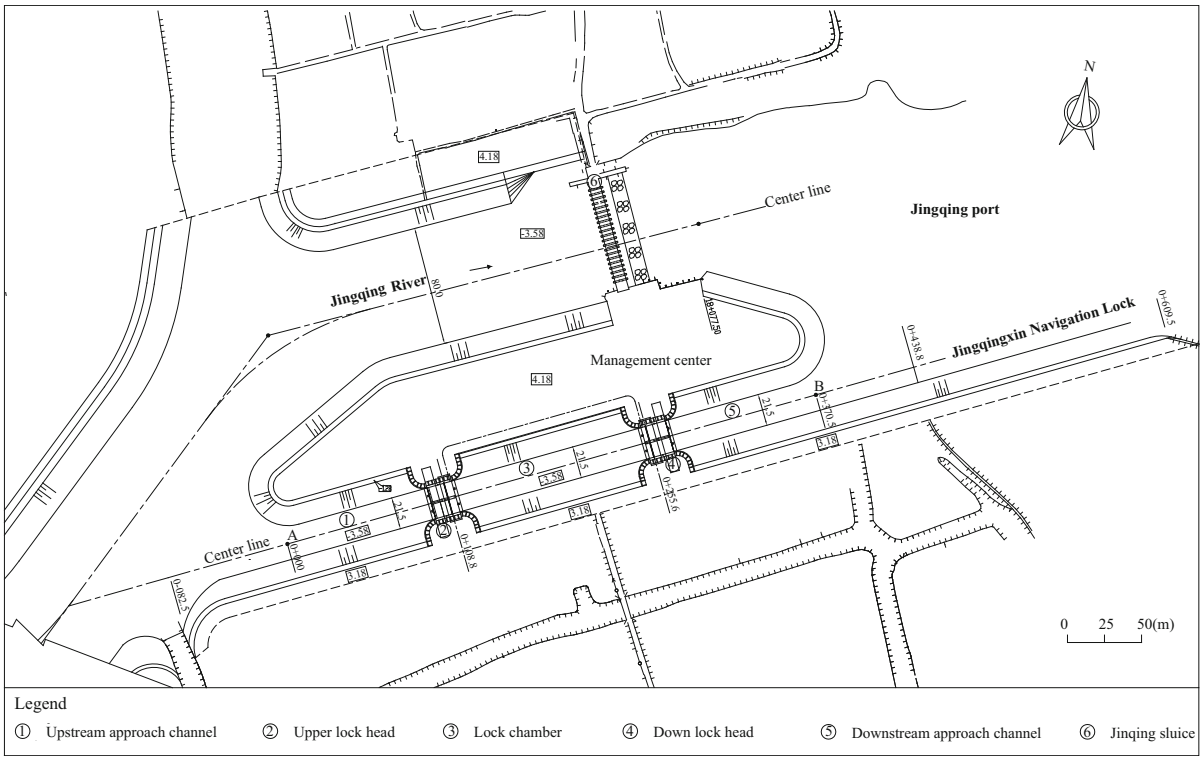

Fig. 2 Plan of the Jingqing navigation lock

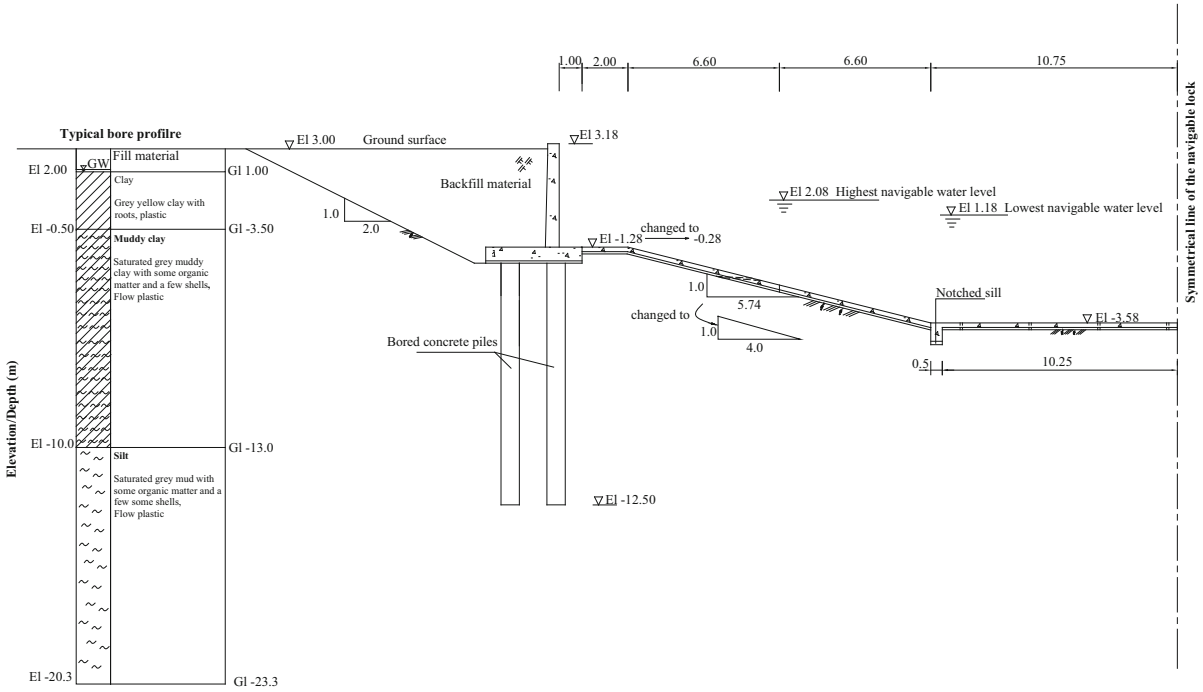

Fig. 3 Geometry of the upper approach channel and corresponding typical soil profile

The width and the elevation of the channel base are 21.5 and −3.58 m, respectively. A 2.0 m wide berm was designed at the elevation of −1.28 m on both bank sides. Beneath and above the berm is a slope 1(V):5.74(H), and a 3.46 m high concrete cantilever retaining walls, respectively. Approximately 1117 bored concrete piles of 12.5 m long and ranged in two longitudinal rows were arranged to support the retaining walls. The diameters of these bored concrete piles are 0.8 m, and the center-to-center spacing between adjacent piles is 2.0 m.

Unfortunately, to reduce the project cost and the height of cantilever retaining wall, the above design arrangement was not followed but changed to a new scheme during the later construction process. Figure 3 also shows the main changes, specifically, the bottom elevation of the berm was changed to −0.28 m, accordingly the slope ratio was changed to 1(V):4.0(H). In addition, the length of the bored piles was changed to 8.0 m.

2.3 Construction Stages

The slope excavation was conducted using the open cut unsupported method. The final excavation grade was at EL −3.58 m, thus the final excavation depth of the basement was 6.08–7.08 m. Meanwhile, the open pumping method, which is widely involved in unsupported excavations with relatively flat slopes, was adopted for dewatering. Water is permitted to flow into the excavation and is subsequently pumped out from sumps and ditches. However, no other dewatering (e.g., deep wells) and slope surface protection measures were accomplished inside the excavation area during the construction process.

To reduce the deflection during the construction, the layered and blocked excavation method was carried out. The slope excavation was 521.4 m long and 61.8 m wide and carried out in five construction sections: Section 1 = upper lock head, Section 2 = down lock head, Section 3 = upstream approach channel, Section 4 = lock chamber, and Section 5 = downstream approach channel (Fig. 4). The construction of the excavation was proceeded from the upper and down lock head to upstream and downstream, i.e., from Section 1 to 4, from Section 2 to 5. Moreover, the bored concrete piles were installed before the slope excavation. For each section, the slope excavation was again successively cut in two phases, in other words, two longitudinal strips by means of the El −0.28 m berm. After the completion of the preliminary excavation, a further cut slope excavation was executed.

Referring to the construction history, the construction stages consists of: (a) install bored pile (60 days), (b) excavation phase 1 (7 days) (Fig. 5), namely excavate to the El −0.28 m berm, and simultaneously arrange the longitudinal drainage ditch, (c) cut pile head, (d) excavation phase 2 (20 days), namely excavate to the El −3.58 m channel basement, and simultaneously arrange the longitudinal drainage ditch, (e) clearing up of the excavation base and placement of the basement reinforcement concrete slab, (f) cast concrete protection slab for the second slope, (g) cast the concrete cantilever retaining walls, (h) backfill the 1st slope behind the concrete cantilever retaining wall with silty clay.

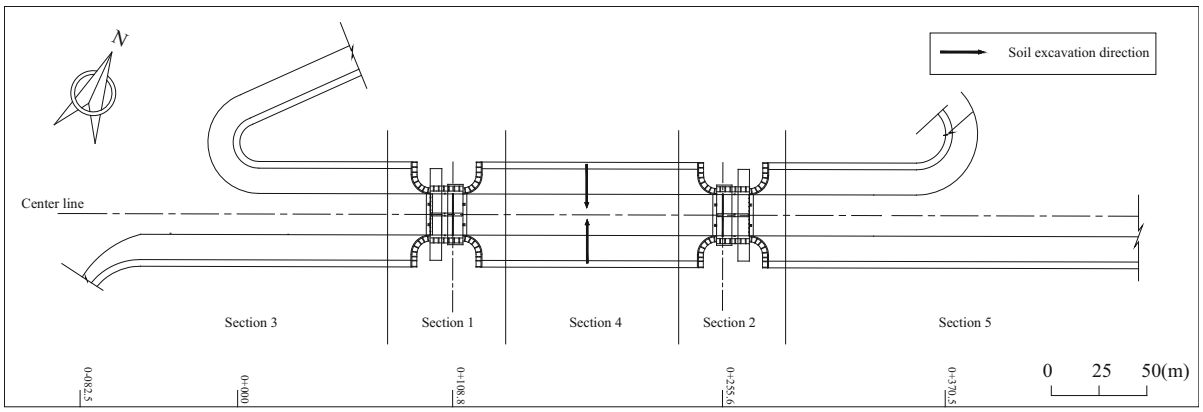

Fig. 4 Construction sequences of the excavation

Fig. 5 View of placement of the bored piles and excavation phase 1

2.4 Slope Collapse

December 13, 2013, the collapse of the excavation occurred. Tension cracks approximately 10 cm wide extending intermittently approximately 90-m long between station 0 + 058 to station 0 + 148 in right in the Section 3 were observed (Figs. 6 and 7). Then some measures such as inserting a wooden propped support and soil reinforcement were taken to stop the situation. Unfortunately, no monitoring instruments were present and thus no monitoring data was available. Approximately 2 weeks before the collapse, moderate rainfall occurred after the completion of the excavation phase 2. Based on the observation of the workers at the excavation site, the top layer was filled with water.

Later, on May 2nd 2014 some similar accidents occurred in the left bank in Section 4 (Fig. 6). The slope collapse led to incline of several bored concrete piles toward the excavation base to some extent.

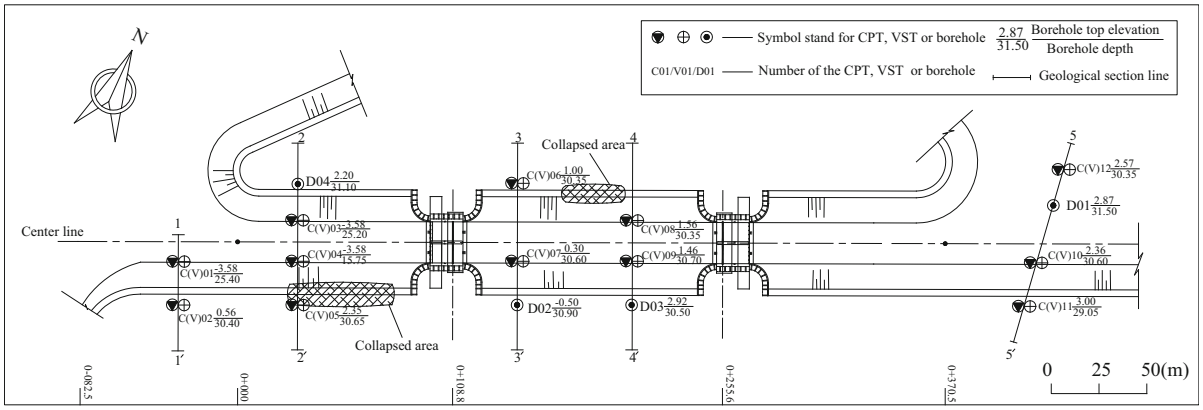

Fig. 6 Collapsed zone, and locations of site reinvestigation

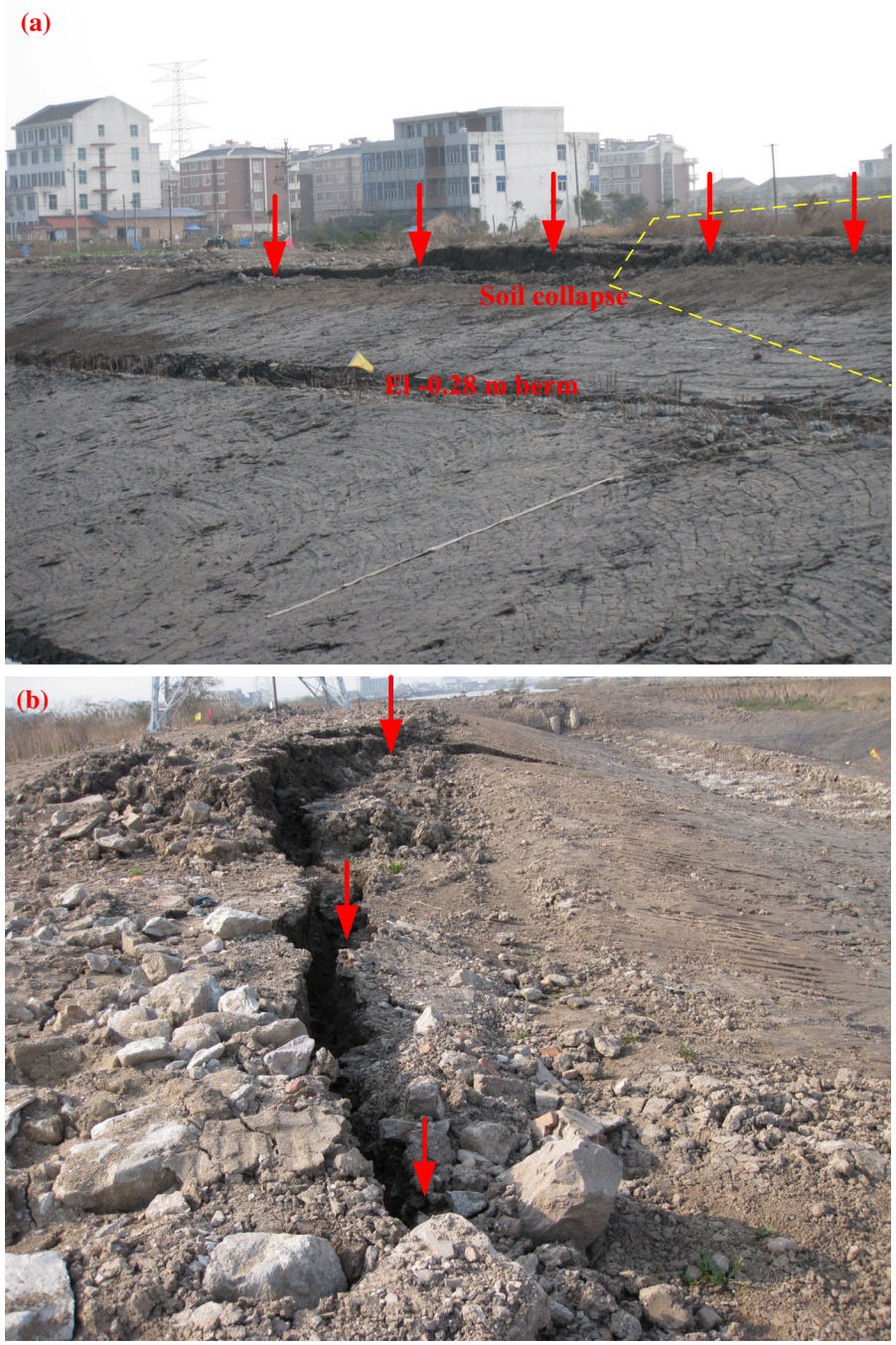

Fig. 7 View of collapse of unprotected slope in Section 3: **a** overview of excavated slope failure; **b** overview of ground tension crack

3 Failure Investigation and Analysis

3.1 Site Reinvestigation after the Collapse

Because the site conditions may be changed due to the rotary drilling for installation of bored piles and a series of soil excavation, a comprehensive site reinvestigation was carried out in order to gain reliable in-situ data after the collapse in January 2015. During the reinvestigation, a series of measurements were employed to investigate the soil properties, including VSTs, CPTs, and standard penetration tests (SPTs) in

the field. Twelve CPTs and twelve VSTs at the site as shown in Fig. 6 were conducted to investigate the undrained shear strength (C_u) of the in-situ soils. Laboratory tests such as consolidated quick direct shear (CQ) tests, and quick direct shear (Q) tests were also conducted.

The physical and mechanical properties of soils within a depth of 30 m at the excavation site can be found in Table 2, while the typical parameters of the soils at borehole D04 are shown in Fig. 8. The variation of the field shear strength C_u with depth at V03, V04, V05, V06, and V07 are presented in Fig. 9. Typical soil profile sections for excavation Sections 3 and 4 are shown in Fig. 10, these sections are identified as Sections 2-2 and 3-3 on the locations of site reinvestigation (Fig. 6).

The main advantage of the VST is that the test itself causes little disturbance to the soil. This is particularly important in sensitive clays. To simulate reasonably, the field VST method has been commonly adopted to determine the undrained shear strength for stability assessment of slope excavations in clayey soils around the rivers and along coastal areas in Southeastern China. However, even with the

Table 2 Soil properties from site reinvestigation after the collapse

Stratum	w (%)	e_0	w_l (%)	w_p (%)	I_p	I_l	k_h (cm/s)	c_v (MPa^{-1})	E_s (MPa)	c_q (kPa)	φ_q (°)	c_{cq} (kPa)	φ_{cq} (°)
II1: mucky clay	49.1	1.344	43.2	23.9	19.3	1.31	8.11e−7	1.090	2.21	6.5	3.4	9.5	14.2
IIsil: muck	56.3	1.548	51.4	27.1	24.2	1.21	1.13e−6	1.241	2.07	8.5	3.2	13.7	13.1
III0: clay	27.0	0.737	32.8	19.7	13.1	0.56	3.48e−7	0.320	5.46	18.6	11.1	20.4	16.1
III3: silty clay	33.2	0.906	33.9	20.1	13.7	0.97	6.35e−7	0.476	4.04	9.6	10.9	13.9	21.4

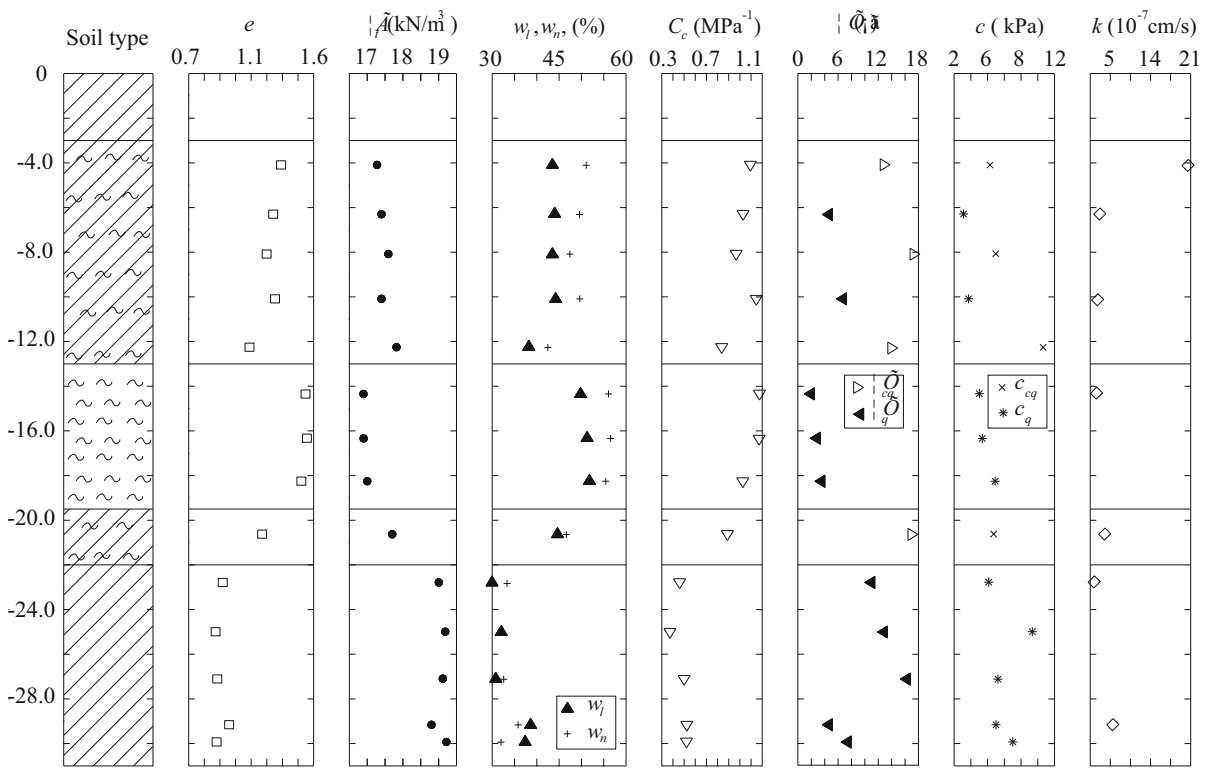

Fig. 8 Physical and mechanical properties of the soils at borehole D04 at the site. *Note*: e, void ratio; γ_t, unit weight; w_l, liquit limit (%); w_n, natural water content (%); φ, angel of internal friction; q, quick direct shear test; cq, consolidated quick direct shear test; c, cohesion; C_c, compression index; k, hydraulic conductivity from laboratory testing, respectively

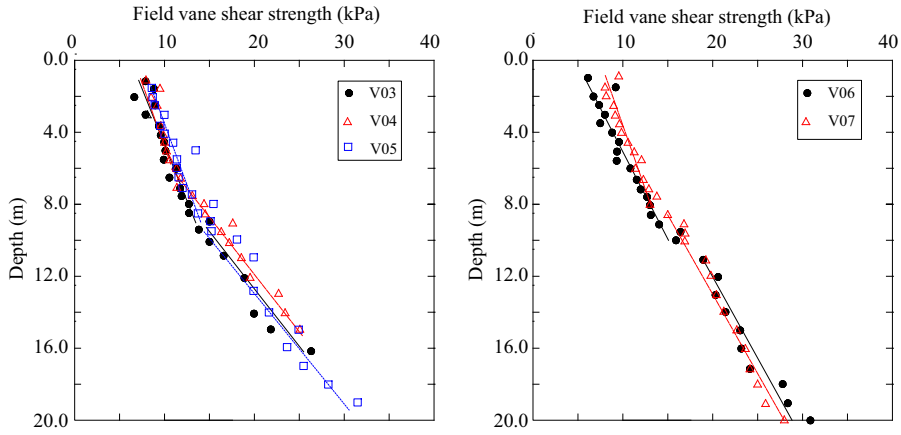

Fig. 9 Variation of field shear strength C_u from VSTs at V03, V04, V05, V06 and V07

use of the field vane shear strength (C_u), the stability state of the slope will not be estimated reasonably (Chung et al. 2012; Ching and Phoon 2013; Yan et al. 2010). This is because the vane shear strength mainly reflects the undrained shear strength of vertical shear face. As a consequence, the safety factor determined from the field vane shear strength may not realistically reflect the actual stability of the slope (Yan et al. 2010). Generally, the undrained shear strength C_u from the VST should be corrected prior to using the undrained shear strength values in the analysis of slope excavation stability.

The shear strength parameters determined from C_u were subjected to statistical regression analysis to take into consideration of the possible effect of non-homogeneity in the soft clay deposit.

Like undrained shear strength obtained from other methods, the C_u of soft clay from the VST varies with depth. For jth (j = 1, 2, …) layer of soft soils, the average depth and the average field vane shear strength C_u can be calculated as

$$\mu_z = \frac{1}{n}\sum_{i=1}^{n} z_i \tag{1}$$

$$\mu_{c_u} = \frac{1}{n}\sum_{i=1}^{n} c_{ui} \tag{2}$$

where z is the depth below the ground face; C_u is the average field vane shear strength, n is the sample number for the jth (j = 1, 2, …) layer of soft soils.

The shearing resistances on the cylindrical vertical surface and horizontal shear surface in the VST are different as below

$$c_{uiv} = K_{0j}\gamma' z \tan\varphi_j + c_j \tag{3}$$

$$c_{uih} = \gamma' z \tan\varphi_j + c_j \tag{4}$$

where c_{uiv} and c_{uih} is respectively shear strengths on vertical and horizontal surfaces, respectively; K_{0j} is the at-rest earth pressure coefficient, and K_{0j} = 0.65 ~ 0.72 for soft soil; U_i is the degree of consolidation; and γ' is the effective unit weight, kN/m^3; φ_j and c_j is respectively the regression values of the internal friction angle (°) and the cohesion (kPa) for the jth (j = 1, 2, …) layer of soft soils.

At failure of VST, the limit equilibrium equation can be expressed as follows

$$T = \frac{1}{2}\pi D^2 H c_{uiv} + \frac{1}{6}\pi D^3 c_{uih} \tag{5}$$

where T is the vane shear torque at failure; D and H is respectively the diameter of the cylinder (i.e. width of the vane blade) (m) and the height of the vane (m).

Substituting Eqs. (3) and (4) into Eq. (5), and then the internal friction angle and cohesion for the Mohr–Coulomb model of jth (j = 1, 2, …) layer of soft soils can be obtained through the linear regression method

$$\hat{c}_u = a\hat{z} + b \tag{6}$$

$$a = \frac{\sum_{i=1}^{n} z_i c_{u_i} - n\mu_z\mu_{c_u}}{\sum_{i=1}^{n}\left(z_i - \mu_z\right)^2} \tag{7}$$

$$b = \mu c_u - a\mu_z \tag{8}$$

$$\varphi_j = \tan^{-1}\left[a \times \frac{H + \frac{1}{3}D}{\left(K_{0j} + \frac{1}{3}D\right)U_t\gamma'}\right] \tag{9}$$

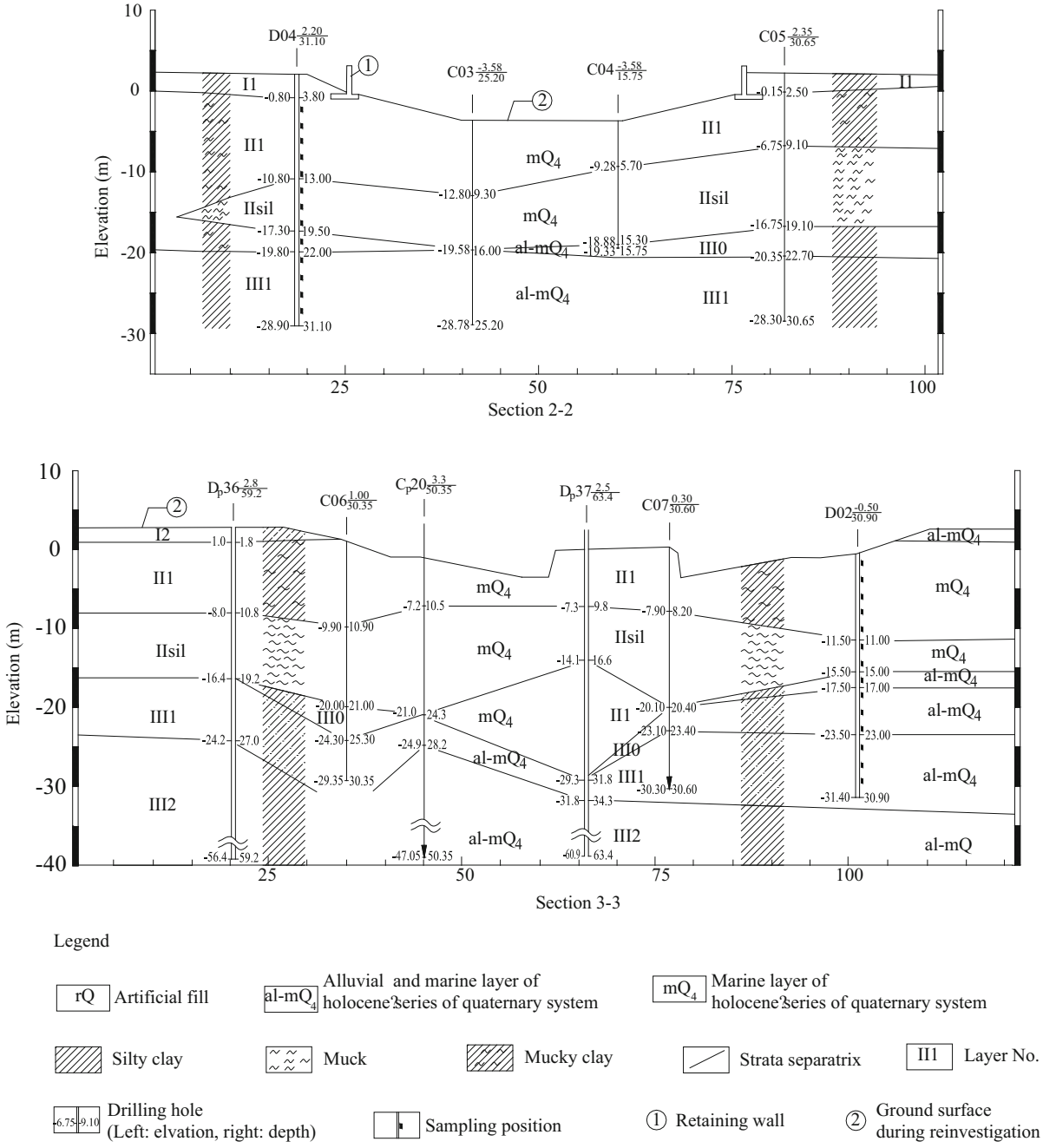

Fig. 10 Typical soil profile sections for excavation Sections 3 and 4

$$c_j = b \tag{10}$$

where a and b is respectively the slope ratio and the intercept of the linear regression equation.

C_u of the concerned soils increases with depth z, which can be expressed respectively by the following equations

$$C_u = 4.36 + 1.08z(\text{kPa}) \quad (\text{for II 1 : mucky clay}) \tag{11}$$

$$C_u = 4.67 + 1.19z(\text{kPa}) \ (\text{for II sil: muck}) \tag{12}$$

The shear strength parameters determined by the above statistical regression method considering the

effect of the shear strength at different orientations. The converted in-situ vane shear strength can be able to estimate the reasonable safety factor of the slope. In the site reinvestigation, rectangular vanes were used for the VSTs, and the size was 100-mm high and 50-mm wide. The strain rate was 0.1–0.2°/s. The C_u of the soils from conducted VSTs was used to determine the corresponding values of the internal friction angle and cohesion for the Mohr–Coulomb model of the layers muck and mucky clay. The results calculated from Eqs. (1) to (7) are listed in Table 3.

3.2 Comparisons of Field Results versus Laboratory Tests

As shown in Fig. 10, the soils within a depth of 30 m can be roughly divided into 3 layers and 6 sub-layers. The top layer I1 is a 0 to 3.0-m-thick fill mainly consisting of grey clay. Below this layer is the 0 to 2.3-m-thick silty clay, namely the second layer I2. The third layer II1 is mucky clay, with its thickness ranging from 5.7 to 19.6 m, and the cone tip resistance q_c is approximately 0.23–0.33 MPa. The next layer IIsil is 4 to 13.8-m-thick muck with decaying organic matter, and its values of q_c ranges from 0.52 to 0.61 MPa. It is the layers of mucky clay and muck that has a predominant effect on the excavation behavior in the case. Below the IIsil layer is the layer III0 and III1, a layer of silty clay with fine sand. The sensitivity index of the predominant clays affecting the excavation mainly, namely the layers of mucky clay and muck, is about 3.0 and 5.0 respectively. These soils can be classified as moderately sensitive clay and very sensitive clays.

Table 3 Parameter values of Mohr–Coulomb model determined by statistical regression method

VST Nos.	II sil: muck		II 1: mucky clay	
	c (kPa)	φ (°)	c (kPa)	φ (°)
V01	5.04	12.17	2.69	14.64
V02	2.54	14.43	4.63	13.09
V04	6.28	8.87	2.22	15.97
V05	5.66	11.35	4.56	13.64
V06	4.82	11.3	4.94	12.97
V07	6.25	10.25	6.02	11.55
V10	3.08	13.81	6.23	11.95
V11	2.74	12.83	1.64	12.7

On the whole, comparing the physical and mechanical parameters in the original design (Table 1) with those from the site reinvestigation (Table 2), it is found that the physical and mechanical parameters of the soils obtained from traditional laboratory tests in the original design phase and the reinvestigation phase were generally consistent with each other.

When compared in terms of laboratory tests for the predominant two soil layers (Tables 1 and 2), the laboratory shear strengths for origin design are identical to the reinvestigation at the project site. Comparing the results from field VST results versus laboratory tests (Tables 1, 2 and 3), the cohesion c in quick direct shear test is higher than the field vane strength while the friction angle φ is much lower. Compared consolidated quick direct shear test with field VST, the cohesion c in quick direct shear test is much lower than the field vane strength while the internal friction angle φ is slightly lower. In other words, the internal friction angle φ of the field vane shear strength is intermediate between compression and these two types of laboratory tests, and the cohesion c is lower than those. The field VST results also imply that the strength of the soft clay would degrade substantially once it is subjected to disturbances arising from construction activities. On this basis, it could be concluded that for these two soil layers were disturbed to some extent because of the effect of the boring holes for bored concrete piles and the cut slope.

In addition, as shown in Fig. 10, it should be noted that the boring logs actually show significant variations in the thickness of the individual strata across the site, reflecting the complexity of the geology.

3.3 Stability Assessment of the Slope Excavation

The main aim of the slope excavation analysis is to estimate the safety during the construction process. An accurate evaluation of this type of stability is intimately dependent upon the applied analysis method and the representation of soil shear strength given as an input (Chenari and Zamanzadeh 2016). Undrained shear strength as measured by field VST is commonly used as an input for soil shear strength parameters of slope stability analyses for the excavation.

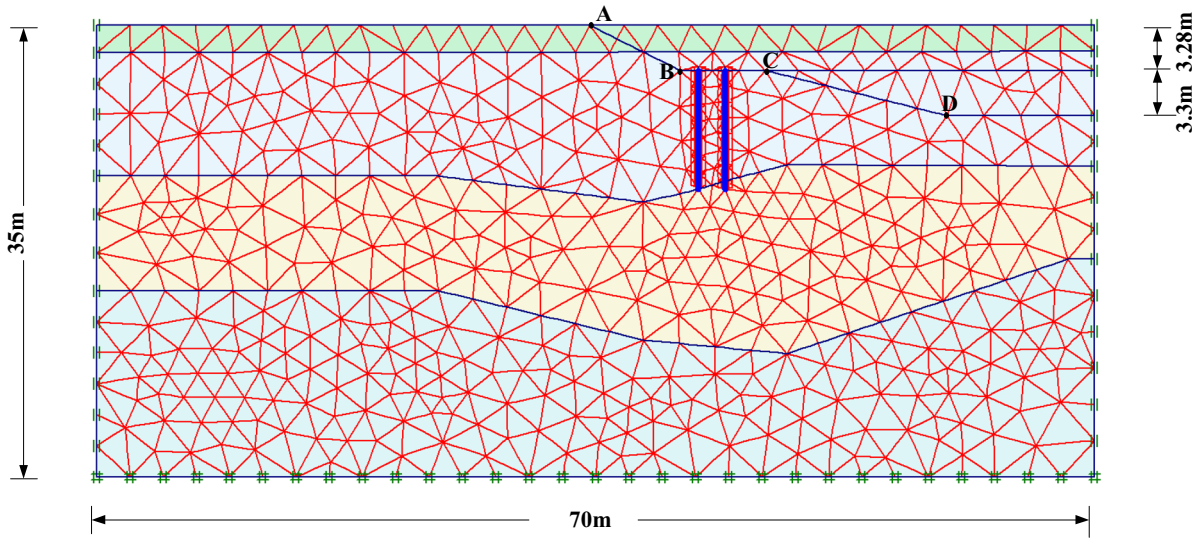

Fig. 11 FEM mesh and boundary conditions

3.3.1 Mesh and Boundary Conditions

As the ratio of the length (L) to width (B) of the excavation was high ($L/B = 8.44$), the 3D effect along the long sides was small (Likitlersuang et al. 2013); thus a widely used commercial FEM program, PLAXIS2D, was used to assess the performance and the FOS of the deep cut open slope excavation during the construction process. A plane strain condition was assumed for the FEM analysis. The 2D plane strain finite analysis approach, using PLAXIS v.9 software (PLAXIS2D v.9, 2009), was adopted in this study. The cross section passing through a given profile (shown in Fig. 10b) was selected to increase analysis accuracy. Figure 11 shows the finite-element mesh used for analysis in which the right boundary is set at the center of the excavation. Considering the symmetry of the excavation, the left boundary was set at the distance of 70 m from the excavation center line, which is beyond the excavation influence zone, usually larger than four times the excavation depth. The bottom was set at the silty clay with fine sand level, e.g., 35 m below the ground surface, which is a silty clay layer. The left and right vertical boundaries are restrained from the horizontal movement and the bottom is restrained from both the vertical and horizontal movements. The drainage boundary condition at the ground surface was drained, and along the two vertical mesh boundaries and at the bottom boundary it was undrained. In this study, the large deformation phenomenon was considered by updating the nodal coordinates after each load. All soil layers were modeled using 15-node elements. The model has an average element size of 1.55 m and a total element number of 1000. The updated Lagarangian formulation, the so-called relative description, is adopted to describe the deformation of the finite element mesh in which a current mesh configuration, and is treated as the reference mesh configuration for the description of the past and future mesh configurations. In addition, the finite element model for the original scheme before change was also established to compare with the adopted one.

In this study, the slope stability analyses incorporate rainfall influences by only changing the groundwater with increasing pressure heads and a rising groundwater table. For this elongated slope, it is assumed that the groundwater table was parallel to the ground surface and fluctuated between 0.5 m below it. The soil strata were likely to behave in an undrained condition and the total excavation period of several weeks (or few months) is typically not long enough to establish steady-state seepage flow in mucky clay and muck. Therefore, the soil parameters that were derived in undrained condition were more relevant for numerical analysis. To assess the behavior of soil in short-term (undrained) condition in deep excavation problem, the typical practice is to perform plastic calculation with undrained material followed by safety factor type analysis.

Table 4 Input parameters of subsoil used in FEM

Stratum	γ (kN/m^3)	k_v (cm/s)	k_h (cm/s)	E (MPa)	Consolidated quick direct shear test		Field vane shear test		Field vane shear test
					c_{cq} (kPa)	φ_{cq} (°)	c (kPa)	φ (°)	C_u (kPa)
I2: clay	18.0	1.39e−6	1.12e−6	2.69	25.0	17.0			
II1: mucky clay	17.6	1.90e−6	3.04e−6	2.05	10.3	14.6	4.1	13.3	$4.4 + 1.1\ z$
IIsil: muck	16.9	4.54e−7	6.65e−6	1.95	13.9	13.6	4.6	11.9	$4.76 + 1.2\ z$
III1: silty clay	20.8	8.82e−6	6.14e−5	5.06	20.4	16.1			

3.3.2 Constitutive Model and Parameters

The Mohr–Coulomb model is an elastic perfectly plastic model, and in fact a combination of Hooke's law and the generalized form of Coulomb's failure criterion. The stress–strain behavior of the soft soil was modeled by Mohr–Column Model (MCM). This is because the yield or failure behavior of the soil is of interest in this study, and the MCM for clayey soils has been widely used in geotechnical engineering practice (Yildiz and Uysal 2015). The model requires five input parameters, namely, the two pseudoelastic parameters from Hooke's law (Young's modulus, E, and Poisson's ratio, υ), and the three parameters from Coulomb's failure criterion (the internal friction angle φ, cohesion c, and dilatancy angle Ψ). With the total stress analysis, the undrained Poisson's ratio υ and dilatancy angle Ψ should be equal to 0.495 and 0 respectively for the saturated soft soil under the undrained condition.

The shear strength parameters used in this study are listed associated with the testing types in Table 4. As listed in Table 4, various parameter combinations associated with corresponding test types were adopted to predict the performance of the excavation. In addition, for VST in reinvestigation, both the regressed parameters and the field shear strength C_u were analyzed. In the later condition, the cohesion intercept should be equal to the field undrained shear strength C_u, and the friction angle is equal to 0.

For the structural component (i.e., bored concrete piles), zero-thickness plate elements were used, in which the linear-elastic model was assumed. The interaction between the pile and soils was simulated with interface elements whose behaviors follow the MCM. The strength parameters (c_i and f_i) of interfaces were calculated from those of corresponding soils with the application of strength reduction factor. The values of the strength reduction factors were roughly taken at 0.80 for both mucky clay and muck. The axial stiffness (EA) and the flexural rigidity (EI) of the bored piles was estimated from the compressive strength of the concrete, considering the possibility of bending moment-induced crack in the pile and the relatively low quality of concreting in water. The equivalent area method was used to simplify the pile into a two-dimensional plane-strain model by applying

$$EA = E_{\text{pile}} A_{\text{pile}} / s \tag{13}$$

$$EI = E_{\text{pile}} I_{\text{pile}} / s \tag{14}$$

where E_{pile} and I_{pile} is the equivalent Young's modulus and of the bored pile, and E was reduced by 20%, A_{pile} is the area of the pile, s is the center-to-center distance in the direction perpendicular to the plane of the embankment cross section.

Followed by plastic calculation with undrained material, the safety factor type analysis was carried out. The FOS assessment of the excavation was conducted using the shear strength reduction technique performed in the convergence criterion method (Su et al. 2015). Failure is defined when no convergence of numerical solutions in the calculation occurs, and the corresponding strength reduction ratio value is treated as the FOS of excavations. Therefore, in stability analysis of an excavation, the strength reduction procedure will be performed by simultaneously applying the same strength reduction to both c and tanφ as follows

$$c_{\text{reduced}} = \frac{c_{\text{input}}}{\text{FOS}} \tag{15}$$

$$\tan \varphi_{\text{reduced}} = \frac{\tan \varphi_{\text{input}}}{\text{FOS}} \tag{16}$$

It is assumed that there is no influence by the reduction in shear strength parameters of soil on the deformation parameters.

3.3.3 Results and Analysis

The effect of key input parameters on excavation behavior and FOS of open cut excavations were studied. Five slope stability analyses were conducted by considering different soil properties listed in Table 4 and geometries of original design and later adopted schemes. These five cases are as follows. Case-1 may be regarded as an original design scheme and soil properties, while Case-2 was conducted to investigate the effect of the geometry change, Case-3 was the same as Case-2 except it was assumed that the soil properties was those obtained from corrected results of field VSTs in the above Section 3.1, Case 4 was the same as Case-3 but the input strength parameters used those of C_u as listed in Table 4, based on Case-3, Case-5 was carried out to investigate the influence of the surface surcharge load along the excavation edge.

Figures 12a–e respectively present the predicted lateral displacements changing with construction dates at concerned points A (ground surface), B (berm heel), C (berm toe), and D (excavation bottom) at the cross-section of excavation Section 3 (Fig. 11) for the above five cases. It can be seen that the differences in the predicted lateral displacements and corresponding change trends among these five cases are relatively obvious. For example, the cumulative lateral displacements at point C after 27 days was 0.07, 0.09 and 0.19 m, for Cases 2, 3 and 4 with various input parameter associated with test types. The maximum difference of the calculated results between Cases 3 and 4 is about 111% (0.10 m). What's more, the variation trends of the calculated lateral displacements are evident for Cases 2, 3, and 4. It is observed from Figs. 12c and d that the calculation lateral displacements during the excavation to El. −3.58 m for Cases 3 and 4 with field VST test parameters increased exponentially. The discrepancy of results among these cases may be due to possible deviations in laboratory and field test types.

Figures 13a–e show the comparison of FOS among the five cases during construction. The calculated FOS values after the excavation to El. −3.58 m are both 1.51 for Cases 1 and 2. The recommended value for FOS of excavated slope during construction stage is 1.10. For Cases 3 and 4, these FOS values are 1.08 and 1.02 respectively. The FOS analyses results indicate that the excavated slope under the field shear strength was not on the safe side and the FOS of the excavation was insufficient. In addition, for Case 5, this FOS value gives 1.03, which indicates that the excavated slope was easily collapsed under the trigger of environmental loads and factors.

For Case 4, the distribution of plastic points as a shear strength reduction ratio equal to 1.02 is presented in Fig. 14. The Mohr–Coulomb plastic points indicate that the Coulomb failure is reached for these points, while the tension cutoff points imply that the tension cutoff criterion is applied. Figure 15 shows the incremental lateral displacements in the last calculation step of the final excavation stage as a shear strength reduction ratio equal to 1.02. As shown in Fig. 14, the plastic points develop at the ground surface and most of the soils of mucky clay and muck layers of the excavation get into a plastic state. The location of the tension cutoff points implies the position of ground cracks. It can be seen that the ground cracks were at the locations along or near the excavation edge of the Section 3. The predicted position of the ground cracks from the FEM analysis results were generally consistent with the fact that the ground cracks at the Section 3 excavation site as shown in Figs. 7 and 14, hence the FEM performs well in predicting the excavation behavior with the field undrained shear strength.

3.4 Failure Mechanism Discussion

Through the field investigation and numerical analysis, the reasons leading to the collapse of the excavation can be summarized as follows:

The layers of mucky clay and muck within the depth of GL −20.0 m are the predominate soils affecting the cut slope excavation owing to the considerably high compressibility, high sensitivity, high viscosity, high liquidity index, and low shear strength. In the condition of determined geometry, the stability is dependent on the in-situ undrained strength of the soft soil. However, it is found that the cohesion c and the friction angle φ used in the original design were higher than those from the field VST of reinvestigation. Based on the comparison of the undrained shear strength of the in-situ VSTs and those of laboratory tests, it is found that the soft soil of layers of mucky clay and muck were disturbed because of the effect of the rotary drilling for bored concrete piles and stress relief of the cut slope. The actual shear strength is less than that used in the original design.

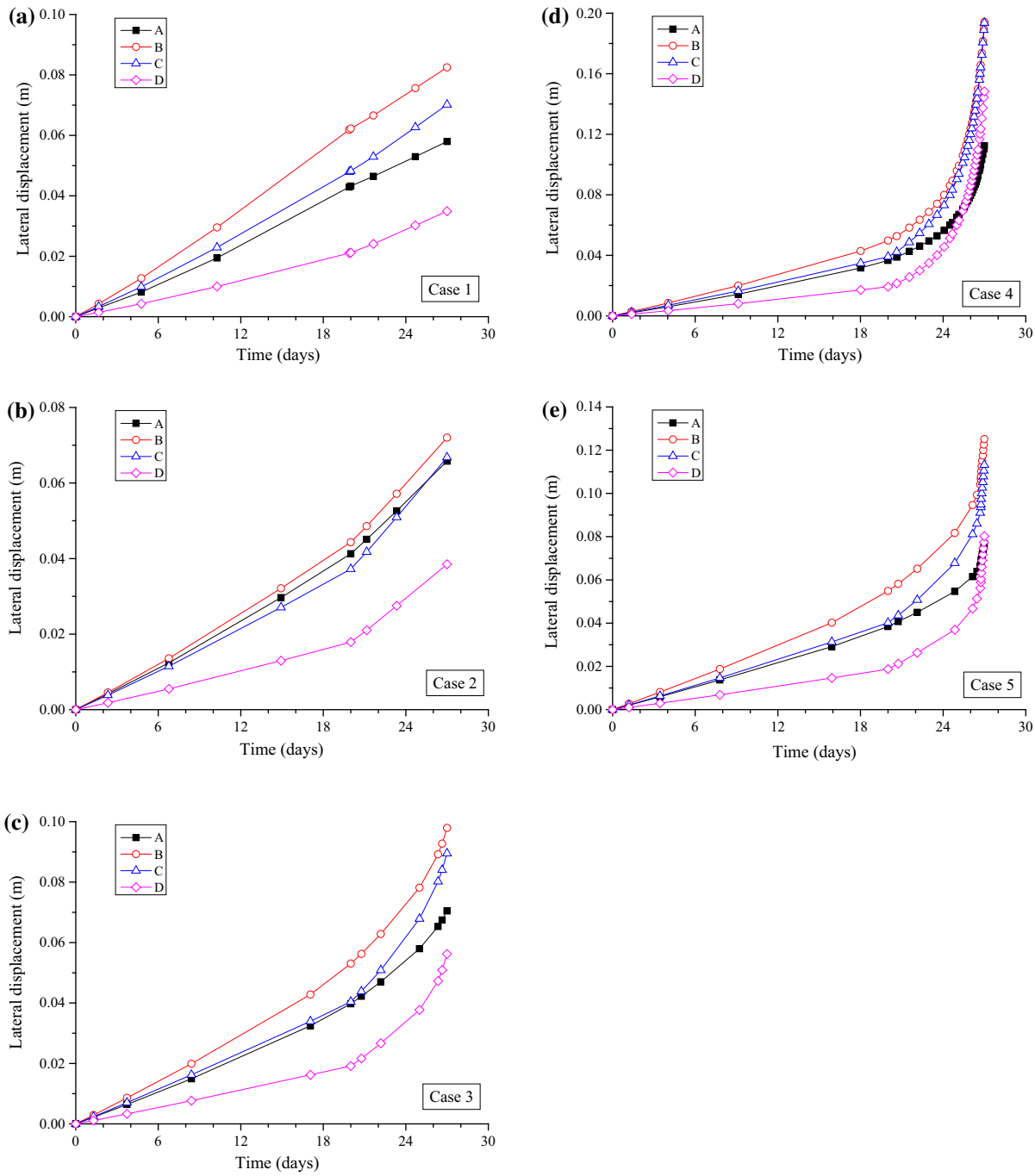

Fig. 12 Variation of deformation with different soil properties associated with test types and geometries: **a** case 1, **b** case 2, **c** case 3, **d** case 4, **e** case 5

An unsupported cut with free slopes in soft cohesive soils are limited to very shallow depths. Generally, the limited depth is 3.0 m (Kempfert and Gebreselassie 2006). The FEM analyses results using PLAXIS 2D indicates that misuse of soil properties causes a decrease of FOS for these cut unsupported excavation.

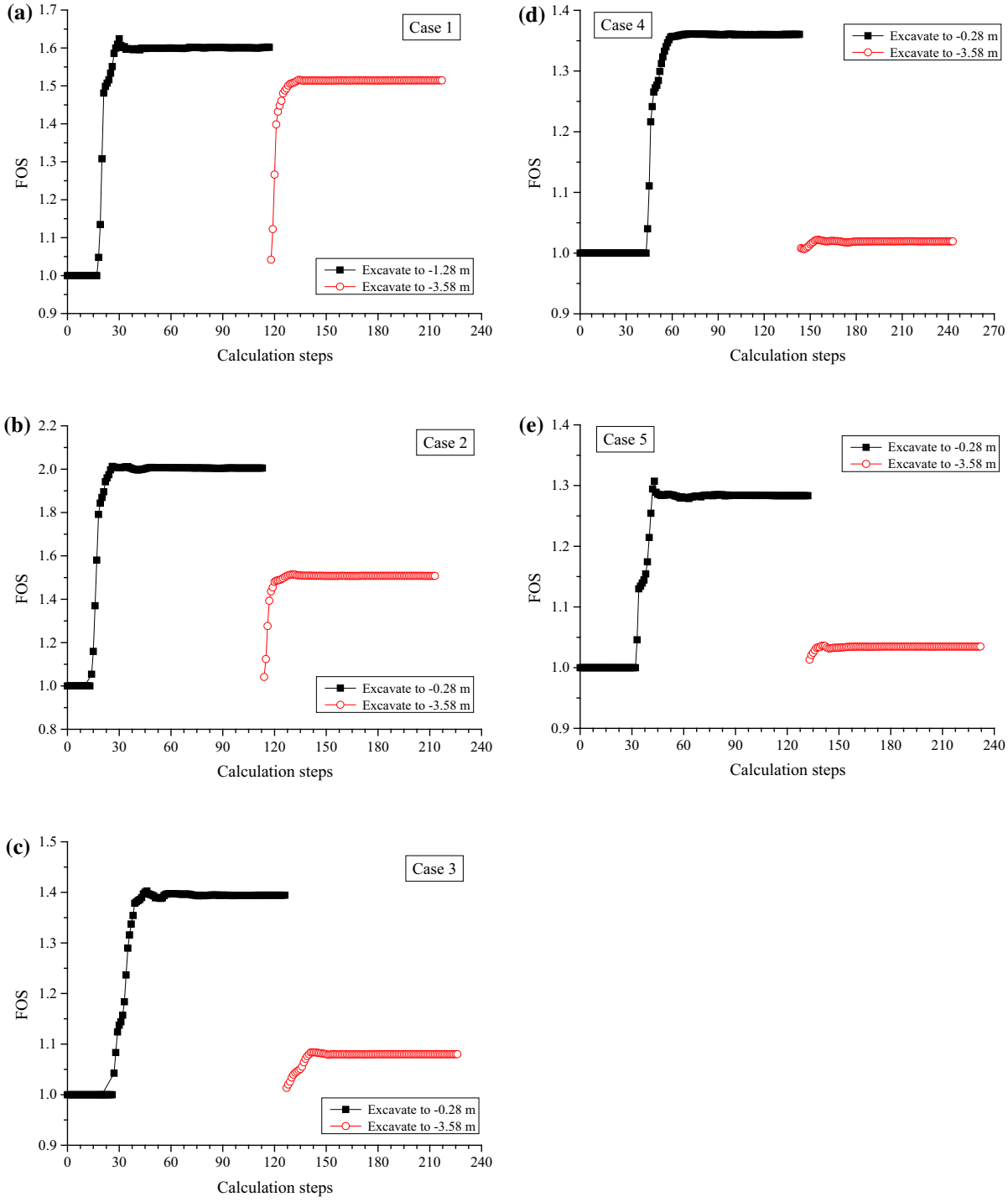

Fig. 13 Effect of soil properties on FOS of excavation: **a** case 1, **b** case 2, **c** case 3, **d** case 4, **e** case 5

Under design of the slope caused insufficient FOS at the excavation. In addition, the bored piles serve as load bearing slab to prevent the slope failure.

Unsupported excavations require protection using different techniques, such as slope protection, vacuum drainage, filter layer, etc. (Kempfert and Gebreselassie

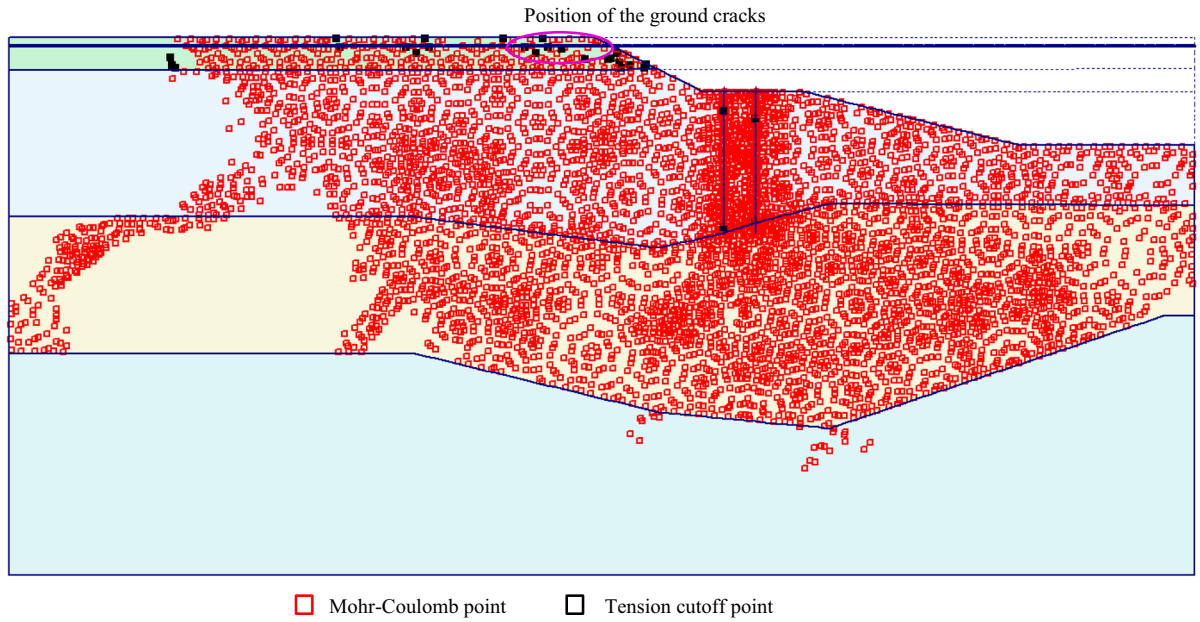

Fig. 14 Distribution of the plastic points as shear strength reduction ratio equals 1.02 for case 4

2006). From Fig. 5, it is observed that no slope protection and drainage measures were taken. What's more, approximately 2 weeks before the collapse, moderate rainfall occurred. Based on the observation of the workers at the excavation site, the top layer was filled with water. The failure is related to ground water and rainfall. Failure can also relate to the decrease in shear strength caused by the loss of suction.

Based on the failure investigation and FEM analysis, the reasons of excavation collapse can be considered as the misuse of soil properties, and inadequate construction management.

4 Lessons from the Failure

Through the investigation of the collapse of the slope excavation, a few lessons can be learned as follows:

First, for areas around the rivers and along coastal areas in Southeastern China, where the soil has strong structural property and displays high sensitivity (the sensitivity index is about 5.0 and 3.0 for muck and mucky clay in this study area), a large cut excavation with free slopes in soft cohesive soils should be cautious, verification of the safety of the sloped excavation is necessary. The laboratory triaxial tests are not reliable types of tests for determining the shear parameters of high structured soft soils, because such soils are sensitive to sample disturbance and the restraining effect of the rubber membrane enclosing a triaxial specimen, which contributes to resistance offered against compression and cannot simulate the field condition of soft soil well. In addition, the installation of bored piles can induce significant movements in the surrounding soil in the field. Thus parameters partially under designer control, the design must have sufficient factors of safety to cater for the decrease of in-situ shear strength due to the construction disturbance. Once the deviation of the strength parameters of laboratory tests from empirical values from local projects is found, the parameters used in design should be modified for safety. Numerical modeling can be used to check the design. The effect of disturbance on the stability of a deep cut open slope should not be neglected during the design process. In addition, the design change should be more cautious, and must be well undertaken by competent engineers before the construction implementation.

Second, the hazards and risks during the construction should be identified and corresponding measures should be proposed to withstand them. The moisture content has a significant effect on the undrained shear strength and parameters of soil, cohesive strength and internal friction angle of vary with the quadratic

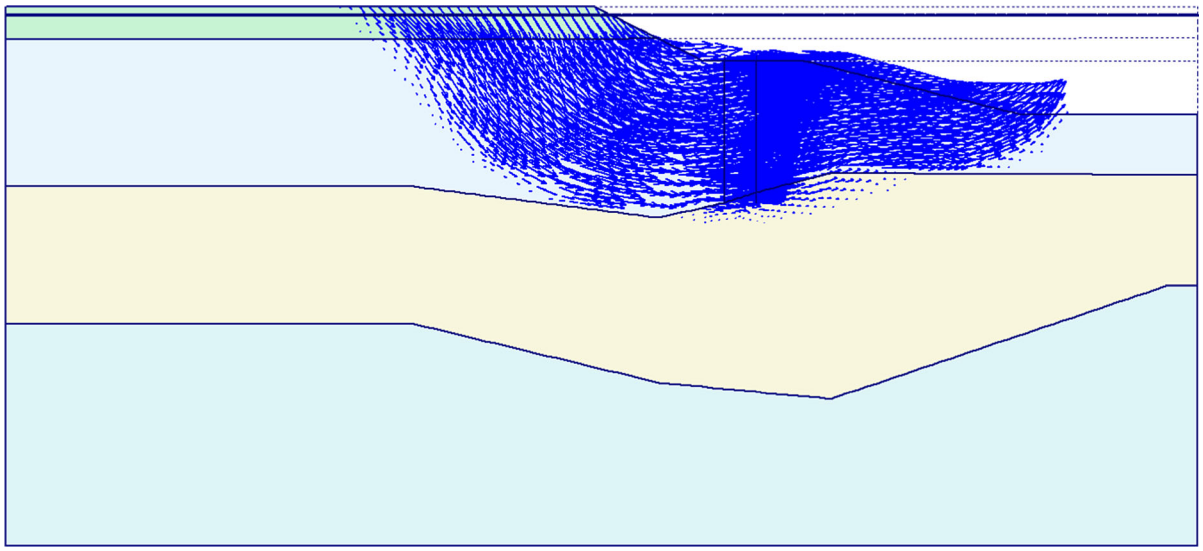

Fig. 15 Incremental lateral displacements in the last calculation step as a shear strength reduction ratio equal to 1.02 for case 4 after excavation

trinomial of moisture content and decrease with the increase of moisture content. More than 90% collapses of excavation occur due to rainfall infiltrating or during a certain time after the rainfall (Hung and Phienwej 2016; Keawsawasvong and Ukritchon 2017). With the rain infiltration the soil saturation and pore water pressure increase, the shallow soil matrix suction decrease or disappear,resulting in the reduction of soil shear strength and decrease of slope stability. Unsupported excavations require protection using different techniques such as slope surface protection (e.g., steel meshed cement mortar, single-grained concrete), drainage measures (e.g., vacuum drainage), etc.

Third, a monitoring system should be appropriately arranged. The monitoring results should be reasonably addressed to meet original design. In particular, monitoring during construction must be meticulously undertaken with an eye to safety.

5 Conclusions

An investigation was conducted to identify the failure mechanism of a deep cut slope excavation on a typical sensitive clay deposit in Southeastern China. According to the shear strength results of the field VST results, traditional laboratory triaxial tests and the numerical simulation analyses of the excavation, the following conclusions can be drawn.

1. The site reinvestigation was conducted after the excavated slope collapses. The field shear strength of the in-situ soils was evaluated based on results from the test data of VSTs. Taking lateral compression coefficient and the average consolidation degree in the soft clay into account, the shear strength parameters obtained by statistical regression analysis with the anisotropy are very close to the field shear strength of soil.
2. Reasonable selection of shear strength of soft soils is generally regarded as the major factor of accuracy in numerical excavation predictions. The corrected shear strength parameters can be used to calculate the slope excavation stability during the construction process. According to the actual environment, the numerical analysis was simplified to fully undrained conditions. The ground cracks were at the locations along or near the excavation edge. The predicted position of the ground cracks from the FEM analysis results were generally consistent with the fact, hence the FEM prediction of the excavation behavior was reasonable and successful. The FOS values are lower than the recommended vale 1.10 and very close to the limited value 1.0. The plastic points develop at the ground surface and most of the soils of mucky

clay and muck layers of the excavation get into a plastic state. The FOS analysis results indicate that the excavated slope under the field shear strength was not on the safe side and the FOS of the excavation was insufficient.

3. The results also indicate that the excavated slope was easily collapsed under the trigger of surface surcharge load and water infiltration. The factors controlling the performance include the shear strength of the soil around and beneath the excavation, the excavation procedure, the groundwater condition, etc.
4. The main reasons leading to the collapse of the excavated slope were discussed and summarized as (1) the misuse of soil shear strength for designers, (2) no slope surface protection measures against rainwater infiltration, (3) no deformation monitoring instruments for early-warning. The investigation of excavation failure mechanism provides the experiences and lessons for unsupported cut with free slopes in soft cohesive soils.

Acknowledgements This research was funded by the National Natural Science Foundation of China (NSFC) (Grant No. 51409167), the Fundamental Research Funds for the Central Public Welfare Research Institute (No. Y716007). The partial data provided by the Construction Headquarter of Jinqingxin Navigation Lock and Zhejiang Design Institute of Water Conservancy and Hydroelectric Power are gratefully acknowledged.

References

Arasan S, Akbulut RK, Isik F, Zaimoglu AS (2016) Behavior of polymer columns in soft clayey soil: a preliminary study. Geomech Eng 10(1):95–107. doi:10.12989/gae.2016.10.1.095

Chen RP, Li ZC, Chen YM, Ou CY, Hu Q, Rao M (2015) Failure investigation at a collapsed deep excavation in very sensitive organic soft clay. J Perform Constr Facil 29:04014078. doi:10.1061/(ASCE)CF.1943-5509.0000557

Chenari RJ, Zamanzadeh M (2016) Uncertainty assessment of critical excavation depth of vertical unsupported cuts in undrained clay using random field theorem. Sci Iran A 23(3):864–875

Ching J, Phoon KK (2013) Multivariate distribution for undrained shear strengths under various test procedures. Can Geotech J 50:907–923. doi:10.1139/cgj-2013-0400

Chung SG, Hong YP, Lee JM, Min SC (2012) Evaluation of the undrained shear strength of Busan clay. KSCE J Civ Eng 16(5):733–741. doi:10.1007/s12205-012-1583-8

Hung K, Phienwej N (2016) Practice and experience in deep excavations in soft soil of Ho Chi Minh city, Vietnam. KSCE J Civ Eng 20(6):2221–2234. doi:10.1007/s12205-015-0470-5

Irfan M, Akbar A, Aziz M, Khan AH (2013) A parametric study on stability of open excavations in alluvial soils of Lahore district, Pakistan. Geotech Geol Eng 31:729–738. doi:10.1007/s10706-013-9623-9

Keawsawasvong S, Ukritchon B (2017) Stability of unsupported conical excavations in non-homogeneous clays. Comput Geotech 81:125–136. doi:10.1016/j.compgeo.2016.08.007

Kempfert HG, Gebreselassie B (2006) Excavations and foundations in soft soils. Springer, Berlin

Likitlersuang S, Surarak C, Wanatowski D, Oh E, Balasubramaniam A (2013) Finite element analysis of a deep excavation: a case study from the Bangkok MRT. Soils Found 53:756–773. doi:10.1016/j.sandf.2013.08.013

Su HZ, Hu J, Yang M (2015) Evaluation method for slope stability under multianchor support. Nat Hazards Rev 16:04014034. doi:10.1061/(ASCE)NH.1527-6996.0000171

Tan Y, Wei B, Zhou X, Diao YP (2015) Lessons learned from construction of Shanghai metro stations: importance of quick excavation, prompt propping, timely casting, and segmented construction. J Perform Constr Facil 29:04014096. doi:10.1061/(ASCE)CF.1943-5509.0000599

Wu HN, Shen SL, Ma L, Yin ZY, Horpibulsuk S (2015) Evaluation of the strength increase of marine clay under staged embankment loading: a case study. Mar Georesour Geotechnol 33:532–541. doi:10.1080/1064119X.2014.954180

Yan S, Feng X, Hou J (2010) Correlating vane shear results with undrained strength parameters for slope stability analysis. In: Liang RY, Zhang F, Yang K (eds) Deep foundations and geotechnical in situ testing, GeoShanghai 2010. American Society of Civil Engineers, Shanghai

Yildiz A, Uysal F (2015) Numerical modelling of Haarajoki test embankment on soft clays with and without PVDs. Geomech Eng 8(5):707–726. doi:10.12989/gae.2015.8.5.707

Zhang GC, Xie N, Tang HM, Zhang L, Wu JP (2015) Survey and cause analyses of ground surface deformation near a foundation pit slope: a case study in the three Gorges area, China. Nat Hazards 75:13–31. doi:10.1007/s11069-014-1261-x